Hair phenotype diversity across Indriidae lemurs

*Elizabeth Tapanes[1], Rachel L. Jacobs[1], Ian Harryman[1], Edward E. Louis Jr.[2], Mitchell T. Irwin[3], Jason M. Kamilar[4,5], Brenda J. Bradley[1]

[1] Center for the Advanced Study of Human Paleobiology, Department of Anthropology, The George Washington University

[2] Conservation Genetics Department, Omaha's Henry Doorly Zoo and Aquarium

[3] Department of Anthropology, Northern Illinois University

[4] Department of Anthropology, University of Massachusetts Amherst

[5] Graduate Program in Organismic and Evolutionary Biology, University of Massachusetts Amherst

*= Corresponding author:

Elizabeth.tapanes@gmail.com

Abstract

Hair (i.e., pelage/fur) is a salient feature of primate (including human) diversity and evolution—serving functions tied to thermoregulation, protection, camouflage, and signaling—but wild primate pelage biology and evolution remain relatively understudied. Specifically, assessing multiple hypotheses across distinct phylogenetic scales is essential but is rarely conducted. We examine whole body hair color and density variation across the Indriidae lemurs (*Avahi*, *Indri*, *Propithecus*)—a lineage that, like humans, exhibits vertical posture (i.e., their whole bodies are vertical to the sun). Our analyses consider multiple phylogenetic scales (family-level, genus-level) and hypotheses (e.g., Gloger's rule, the body cooling hypotheses). Our results show that across the Indriidae family, darker hair is typical in wetter regions (per Gloger's rule). However, within *Propithecus*, dark black hair is common in colder forest regions, which may implicate thermoregulation and is the first empirical evidence of Bogert's rule in mammals. Results also show pelage redness increases in populations exhibiting enhanced color vision and may thus aid conspecific communication in forested environments. Lastly, across Indriidae, we find follicle density on the crown and limbs increases in dry and open environments—rare empirical evidence supporting an early hypothesis on hominin hair evolution. We find an effect of body size on hue (red hair) and hair density but not on brightness (black hair). This study highlights how different selective pressures across distinct phylogenetic scales have likely acted on primate hair evolution. Lastly, since hair does not fossilize, the results of follicle and hair density variation across this clade offer us some potential insight into contextualizing human hair evolution.

Keywords: lemurs, coloration, sifaka, opsins, integument, adaptation

Introduction

Hair (i.e., pelage, fur) is a salient feature of primate diversity and evolution and is the product of natural and sexual selection. Hair has been found to play a role in conspecific signaling (Allen and Higham, 2013), thermoregulation (Fratto and Davis, 2011), camouflage (Hoekstra et al., 2005; Barrett et al., 2019), and to possibly provide protection from pathogens/parasites (Paus & Foitzik, 2004). Across all mammals, primates—including humans—arguably exhibit the most diversity in hair color (e.g., bright reds) and growth patterns (e.g., mustaches) between and within species (Rowe, 1996; Caro, 2005). For example, within Colobinae, some *Colobus* spp. sport a long black and white dorsal cape, and *Pygathrix* spp. are often tri-colored and short-haired (Rowe, 1996). Similarly, human hair color and texture vary throughout the human body, between individuals, between populations, and can be correlated with ancestry and ethnicity (Steggerda and Seibert, 1941; Seibert and Steggerda, 1999; Lasisi et al., 2016). Nevertheless, our knowledge about hair evolution is based mainly on non-primate mammals. Primate hair remains relatively understudied (with some notable exceptions: e.g., (Santana et al., 2012; Allen and Higham, 2013; Kamilar et al., 2013; Rakotonirina et al., 2017; Bell et al., 2021)), with most research taking a macro-scale approach and sampling broadly across the primate order (e.g., all catarrhines).

These previous studies indicate that variation in primate hair color likely evolved in response to multiple distinct but not mutually exclusive pressures associated with ecology, visual systems, activity cycles, and sociality (Santana et al., 2012; Allen and Higham, 2013; Kamilar et al., 2013; Rakotonirina et al., 2017; Bell et al., 2021). For example, across primates, melanic (i.e., black) colors often co-occur with humid regions—which may be due to camouflage, pleiotropy, pathogen resistance, or selection on a related trait (i.e., Gloger's rule) (Kamilar and

Bradley, 2011; Santana et al., 2012, 2013; Bell et al., 2021). However, without accounting for variation within families, genera, and species, other subtle trends or relationships may not be detected. For example, recent work in birds suggests a distinct rule (Bogert's rule) may explain some melanic variation in endotherms depending on the phylogenetic and geographic scale sampled (Bogert, 1949; Delhey et al., 2019). According to Bogert's rule, melanic colors should co-occur with cold regions as dark colors may absorb heat better and aid in thermoregulation (Bogert, 1949; Delhey et al., 2019). However, there is no current empirical evidence for this rule in primates (or any mammals). Yet across human populations, variation in eumelanin exceeds that seen in red, blonde, or lighter hair (Lasisi et al., 2016), which suggests that important biological variation may be identified if the scale of analyses was smaller than previously considered (i.e., within a few populations vs. across all populations) (Norton et al., 2016).

Across non-human primates, red hues (and facial patterning) may act as a means to aid conspecific communication (Santana et al., 2012, 2013; Cuthill et al., 2017; Winters et al., 2019). For example, diurnal activity and the ability to perceive a wider range of colors compared to other mammals may have contributed to the enhanced color diversity in specific primate clades (Bell et al., 2021). However, the evidence for coevolution of hair coloration, specifically red hair and color vision in primates, remains mixed (Fernandez and Morris, 2007; Kamilar et al., 2013). Our understanding of primate hair color may benefit from broader sampling across wild populations and/or analyses conducted on smaller phylogenetic scales.

Similarly, our understanding of pelage density evolution remains limited to extensive macro-scale studies. Across primates, the primary trend is that hair density decreases as body size increases (Schwartz and Rosenblum, 1981; Sandel, 2013). One early hypothesis argued that a reduction in body hair density across hominins coupled to increases in activity level, sweat

glands, sweat production, and a change to a dry savannah environment—may have aided thermoregulation (i.e., "body-cooling hypothesis") (Post et al., 1975; Wheeler, 1992; Jablonski and Chaplin, 2000). Despite various physiological models testing evidence of the body-cooling hypothesis (Schwartz and Rosenblum, 1981; Wheeler, 1992; Chaplin, George, Jablonski, Nina G., Cable, 1994), there is only rare empirical evidence for this phenomenon within primates (Best et al., 2019). There also remains a poor understanding of how hair density in primates may be impacted by other factors, such as climate. Because hair does not preserve in the fossil record, studies on wild primates can provide critical insights into the evolutionary mechanisms underlying one of the most interesting traits among humans.

This study examined whole-body pelage color and hair/follicle density across Indriidae—a diverse clade of lemurs. Since the Indriidae clade varies in critical aspects known to drive primate (including human) hair variation, they make a good proxy for testing multiple hair hypotheses that have not yet been jointly assessed in one study. Our overarching goals were to 1) examine if Indriidae pelage variation varies across distinct phylogenetic scales and 2) determine if multiple, non-exclusive selective pressures can impact the same trait. Specifically, we aimed to jointly assess the impacts of climate, body size, and color vision on hair evolution at distinct phylogenetic scales. Collectively, this family (comprising three genera: nocturnal *Avahi* and diurnal *Indri* and *Propithecus*) inhabits almost every bio-climate of Madagascar (e.g., humid rainforest, temperate forests, open spiny forest, mangroves) (Mittermeier, Russell A. et al., 2010). The hair of the 13 species in our study varies intra- and interspecifically in both color (e.g., melanic, tricolored orange) and growth morphologies (e.g., long silky hairs, short hairs) (Petter and Peyrieras, 1972; Tattersall, 1986; Mittermeier, Russell A. et al., 2010; King et al., 2014; Rakotonirina et al., 2014). Indriidae also vary in body size (≈1km (*Avahi*), ≈3-8km

(*Propithecus*), ≈10km (*Indri*))—and phylogenetic relatedness likely impacts body size evolution (Lehman, 2007). Thus, we specifically (1a\2a) aimed to uncover how climate and body size influences: pelage brightness (i.e., black color), hue (i.e., red color), and hair follicle density across Indriidae and within *Propithecus*. We expected that climate impacts pelage color and density evolution distinctly across different phylogenetic scales. We predicted that body size only impacts hair/follicle density, based on evidence from other primates (Sandel, 2013). Diurnal Indriidae (*Indri* and *Propithecus*) also vary in their color vision. In many species, some females have trichromatic color vision (ability to distinguish reddish and greenish hues), while males and other females are red-green color blind (polymorphic color vision; Jacobs et al., 2017). Although this feature occurs in some other day-active lemurs, Indriidae has been found to exhibit greater genetic variation in color vision across species (Jacobs et al., 2017). Accordingly, we (2b) aimed to understand how this variation in color vision impacts pelage hue in diurnal genera. We predicted that populations with enhanced capacity for trichromatic color vision would have individuals with redder pelage (Sumner and Mollon, 2003). Our results provide critical insight into how multiple variables impact primate hair evolution across scales. Importantly, this family consists solely of vertical clingers and leapers, which means they exhibit upright locomotory posture similar to humans (via bipedal hopping (Schmidt, 2011)). Thus, these results (specifically those on hair density) may provide insight into human hair evolution.

Methods

Hair morphology and body size data collection

We used hair color and density measurements from museum research skins (N_{Total} = 63; N_{Museum} = 59) and living animals in one wild population (N_{Wild} = 4, *P. diadema* from

Tsinjoarivo) (SI 1). Museum samples spanned three museum collections (SI 2). In total, we sampled six *Avahi* populations (Figure 1A), 23 *Propithecus* populations (Figure 1B), and four *Indri* populations (Figure 1C). Our sampling included nocturnal and diurnal genera (Figure 1D) across all significant bioclimatic regions in Madagascar (Figure 1E). Many individuals did not have available age or sex-class data. Hence, we did not test for differences between age classes or sex. Although some preliminary evidence suggests there may be subtle pelage dichromatism, sifakas are unlikely highly sexually dichromatic in terms of coloration. Instead, sifakas exhibit more significant visible variation within sexes (i.e., bimorphism in males) (Lewis & Van Schaik, 2007; Mittermeier et al., 2010; Spriggs, 2017; Tapanes et al., 2018). Measurements of hair from wild sifakas consisted of following the same protocol as museum individuals. We also extracted body length (mm), measured from head to tip of tail, from all individuals as a proxy for body size using Photoshop CC 6. We standardized all measurements using the known length of a ruler in the photos. Wild sifakas were captured for ongoing parallel research using a standard capture protocol established by the Prosimian Biomedical Survey Project (PBSP) Team (used on 750+ lemurs, 16+ sites, and 35+ species since 2000) (Dutton et al., 2003; Irwin et al., 2010). Groups were habituated before capture. The capture team was led by a trained professional, and captures were performed at close range using Pneu-dart 9mm disposable non-barbed darts containing tiletamine/zolazepam (Telazol) for immobilization.

[Figure 1 Here]

<u>Hair coloration collection</u>

We used color-calibrated photographs of all animals (N = 63 individuals; SI 1) and a Canon EOS Rebel SL1/EOS 100D mounted with a Canon EF-S18-55mm f/3.5-5.6 IS STM lens.

We calibrated each image against a color standard with 24 color squares of known reflectance values. The camera color mode was set to 'faithful.' The camera was calibrated with a grey standard to set a manual white balance. All individuals were photographed against dull backgrounds using the adjacent method (Bergman and Beehner, 2008; Kendal et al., 2013). We followed established protocols for calibrating photos in previous studies for both museum and wild specimens (Stevens et al., 2007; 2009).

We used the Red-Green-Blue (RGB) color model and extracted all RGB values using Photoshop CC 6 across 14 body regions. Due to the high degree of variation across the pelage of the *Propithecus* tail, ventral surface, and dorsal surface, we divided measurements of these regions into three quadrants (lower, mid, and upper) (SI 3). If one of these regions was damaged, we took measurements from the center as the “average.” Primate hair occupies a relatively small color space, primarily varying along two axes. The first relates to variation in luminance and exhibits little chromatic variation and is captured by similar red, green, and blue values. Thus, we used RGB averages here as a proxy for 'brightness' in a hair patch to indicate if the hair is white, a shade of grey, or black. The second axis of variation is hue and indicates variation along a red/brown axis and can be captured by a ratio of red to green. The latter is because the green and blue channels are most similar, while the red channel exhibits higher values on average. As the Red-Green ratio increases, hair appears increasingly red (Kamilar et al., 2013). We ran a correlation matrix across color values and removed any that were highly correlated with each other ($r > .90$). This reduced our hair color variables to RGB averages and RG ratios for the (1) crown, (2) cheek, (3) dorsal torso, (4) ventral torso, (5) forelimb, (6) hindlimb, and (7) tail. In total, we collected 882 brightness and 882 hue measurements (63 individuals x 14 sampling regions). Previous work on museum skins indicated no effect of storage time on pelage

coloration from 142 museum skins collected over 100 years (1898 and 1998) (Kamilar et al., 2013).

Hair and follicle density collection

We used a protocol that borrows from dermatological methods and instrumentation, which automates hair density measurements (Avram and Rogers, 2009). We used CompareViewHair® software (STR Technologies) tools combined with a specialized hand-held digital light microscope (ProScope HR2©; Bodelin) with a 100x lens. The software included a built-in procedure for calibrating the lens and software before use. The hair of an animal was parted, and the lens was placed on the skin. A light within the microscope illuminated the skin and provided needed light for subsequently photographing the area. We collected microscopy images (detailing transects of hair follicles and shafts) and compiled semi-automated measurements in the laboratory using this system. We examined two hair morphology properties: hair density (shafts/cm^2) and follicle density (infundibula/cm^2).

We collected three microscopy photos (replicates) from five body regions (SI 4) of each animal (n = 47 individuals) (SI 1) using the hand-held microscope, adhering to a previously established protocol (Bradley et al., 2014). The method provided a visual transect/plot of follicles (i.e., infundibula) and the number of hair shafts emerging from each. We used the 'density tool' in CompareViewHair® software to estimate the number of infundibula per cm^2 (i.e., follicle density). We marked each follicle strand manually and used that number to estimate the final value in any given region (given the specific magnification). However, this protocol assumed that the entire photograph was visible, which was not always the case. Therefore, in our final measurements for 'follicle density,' we used the value the software provided of density per cm^2 and divided it by the visible photo's proportion. Similarly, for our final measurement for 'hair

density,' we used the value the software calculated for density per cm^2 and multiplied it by the average number of hairs emerging from each follicle. In total, we collected 235 hair and 235 follicle density measurements (47 individuals x 5 body regions). Previous work on museum skins shows no effect of storage time on pelage density for skins collected over 100 years (Bradley et al., 2014).

Climatic and phylogenetic data collection

We collected climate and environmental data from 33 sampling locations across Madagascar (Figure 1). Specifically, we extracted data from WorldClim (version 1) that consisted of averages from 1960 to 1990. This likely created some noise in the data given museum data spanned the early 1900s to late 1990s. However, sifaka generation times are long (~20 years)—thus, the data are likely representative of accurate averages across bioclimates and phenotypes. Localities were obtained from museum records, and we used Google Earth to obtain geographic coordinates of the nearest forested area in the species range. Localities were listed as forests or towns with directional coordinates (e.g., 40 km W of Tamatave). We used R packages 'raster' and 'sp' to extract all localities' climate data in the WorldClim database (Pebesma and Bavand, n.d.; Hijmans and Etten, 2012). We ran a correlation matrix for all 19 bioclimatic variables and removed any highly correlated variables ($r > .80$). In the end, we used five bioclimatic variables in our comparative analysis as predictor variables (SI 5).

DNA extractions for opsin genotypes

We categorized diurnal Indriidae color vision status (e.g., polymorphic color vision, dichromatic – red-green colorblind) based on X-linked opsin genotypes (Jacobs et al., 2017,

210 2019). Our analysis included diurnal Indriidae represented by a subset of species/populations for
211 which pelage data were also available ($N_{species}$ = 7; $N_{populations}$ = 10; SI 6). Opsin genotypes for
212 populations of diademed sifaka (*Propithecus diadema*), Milne-Edwards's sifaka (*Propithecus*
213 *edwardsi*), golden crowned sifaka (*Propithecus tattersalli*), Verreaux's sifaka (*Propithecus*
214 *verreauxi*), and *Indri indri* were previously published (Jacobs et al., 2017). Data for the silky
215 sifaka (*Propithecus candidus*) and Perrier's sifaka (*Propithecus perrieri*) were based on opsin
216 genotypes obtained from five individuals from Anjanaharibe-Sud ($N_{X\ chromosomes}$ = 8) and
217 Analamera ($N_{X\ chromosomes}$ = 8) populations, respectively, following (Jacobs et al., 2019). Briefly,
218 we extracted genomic DNA from blood/tissue samples using phenol-chloroform-isoamyl
219 extraction protocols (Sambrook et al., 1989). We used quantitative PCR (Mic qPCR Cycler, Bio
220 Molecular Systems; Rotor-Gene Q, Qiagen) to amplify exons 3 and 5 of the X-linked opsin gene.
221 Amplification was followed by high-resolution melt analysis (HRMA) (*following* (Jacobs et al.,
222 2016)), and we determined genotypes for each exon based on the observed melt curve shape and
223 temperature compared to positive controls ($N_{Replicates}$ = 2 per exon). To further confirm genotype
224 calls, we Sanger sequenced qPCR amplicons from at least two individuals representing each
225 observed melt curve. All sequences matched scored genotypes based on melt curves.
226 We estimated the peak spectral sensitivity of observed opsin alleles in each population
227 (*following* (Jacobs et al., 2017)) and determined the difference between the two alleles with
228 maximum and minimum peak spectral sensitivities. These values, along with a total number of
229 observed alleles, were used in downstream analyses as proxies for enhanced trichromatic color
230 vision. Trichromatic color vision is most optimal with more widely separated photopigments
231 (e.g., (Osorio et al., 2004)). A greater number of opsin alleles results in an increased proportion
232 of trichromatic individuals in a population.

233

234 *Analyses*

235

236 Climate and body size effects on pelage brightness and hue

237 We conducted four principal component analyses (PCAs): two across Indriidae and two
238 within *Propithecus*. One was for all the brightness variables across body regions and a second for
239 all the hue variables across body regions for Indriidae, to test specific hypotheses related to each
240 and to reduce the dimensionality of the data. We then ran two additional albeit similar PCAs
241 within only the *Propithecus* genus—given that the *Propithecus* genus is more widely
242 geographically distributed than either *Avahi* or *Indri*. We removed any variables with strongly
243 correlated vectors in the PCAs and then re-ran them to obtain the final PC values. We only used
244 the resulting PC values with eigenvalues over one as our dependent variables.

245 To test the effects of climate on pelage color while accounting for the evolutionary
246 relatedness of taxa, we used phylogenetic generalized linear mixed models (PGLMM) using
247 Markov chain Monte Carlo algorithms (MCMC) via the 'MCMCglmm' package in R (Hadfield,
248 2010). Our Indriidae phylogeny was based on a previously published lemur phylogeny that
249 contains a complete picture of Indriidae evolution (Herrera and Dávalos, 2016). We assigned the
250 phylogeny to the 'pedigree' argument in MCMCglmm, and the resulting matrix was used to
251 weigh the error structure of the model. Similar methodologies have been used to test the effects
252 of climate variables on bumblebee body size (Ramírez-Delgado et al., 2016) and frog vocal
253 signals (McLean et al., 2013). Each model included one color (or hair density) PC value as the
254 dependent variable and the bioclimatic variables (SI 5) and body size as independent variables,
255 with species and phylogeny considered random factors. We log-transformed PC values,

256 bioclimatic variables, and body size to achieve normality. All models ran for 5,000,000 iterations
257 after a burn-in of 500,000 iterations and a thinning interval of 500 using flat priors. We assured
258 effective sampling sizes were adequate for all our models (i.e., ESS virtually equal to MCMC
259 sample size) (Villemereuil and Nakagawa, 2014).

260 We assigned statistical significance when pMCMC ≤ 0.05 (which is equivalent to a p-
261 value (Villemereuil and Nakagawa, 2014)) and when the confidence interval for a given variable
262 did not include zero (Ramírez-Delgado et al., 2016). To estimate what fraction of the pelage
263 variation was attributable to phylogenetic relatedness, we calculated H^2 from Lynch (Lynch,
264 1991) (equivalent to Pagels's λ) which corresponds to the degree of variation in a given trait
265 attributable to phylogenetic relatedness (Hansen and Orzack, 2005; Kamilar and Cooper, 2013).
266 We ran the models across the whole Indriidae family and within the *Propithecus* genus. Using
267 G*Power analysis (Faul et al., 2009), we estimated the PGLMMs would detect a small effect
268 ((Indriidae, 0.25)-(*Propithecus*, 0.35)) with ≈80% power.

269

270 <u>Climate and body size effects on pelage density</u>

271 We conducted two principal component analyses (PCA) of hair and follicle density
272 values: one across all Indriidae taxa and a second within the *Propithecus* genus. We removed any
273 variables whose vectors strongly correlated in each of the PCAs. We used the resulting PC
274 values with eigenvalues over one as dependent variables in our PGLMM models, following the
275 methodology outlined above (see: climate and body size effects on pelage brightness and hue).
276 Using G*Power analysis (Faul et al., 2009), we estimated the Indriidae PGLMM would detect a
277 small effect (0.35), and the *Propithecus* PGLMM would detect a moderate effect (0.50) with
278 ≈80% power. We also conducted an Analysis of Variance (ANOVA) to test for differences

between hair or follicle density across distinct body parts.

Polymorphic trichromacy and pelage hue variation

We ran one PCA on hue variables among a subset of individuals from which we had paired opsin genotypes and pelage measurements from the same population. We used any PCs with eigenvalues over one as the dependent variable in our linear models. To estimate the relationship between pelage hue and color vision, we conducted both (1) a simple linear regression and (2) PGLMM. Due to the small sample size (n = 10 localities/populations) (SI 6), we assumed that the "true" result likely fell between a model where lambda = 0 (simple linear model) and one where lambda = 1 (PGLMM). We followed the methods described previously, except we used 'spectral sensitivity range' (i.e., difference in opsin spectral sensitivity) and the 'total number of opsin alleles' as our independent variables. Despite the low sample size, using G*Power analysis (Faul et al., 2009), we estimated the simple linear model would detect a moderate effect (0.65) with ≈80% power.

Results

Climate and body size effects on pelage brightness and hue

Across Indriidae

Across Indriidae, the first PC for the brightness PCA explained ≈61% of the variation (SI 7). The highest loadings on PC1 were hindlimb, tail, and cheek brightness (SI 8). We found a statistically significant and positive association between hair brightness and precipitation seasonality (Table 1). Thus, darker pelage across Indriidae is associated with forests of lower

precipitation seasonality (i.e., higher rainfall, more humid) (Figure 2A). Brightness across Indriidae exhibited a moderate phylogenetic signal (0.68) (Table 1). On the hue PCA, the first two PCs explained ≈53% of the variation (SI 9, SI 10). The highest loadings were hindlimb, crown and cheek hue (PC1), as well as cheek and dorsal torso hue (PC2) (SI 10). We found a statistically significant relationship between PC2 and temperature annual range (Table 2). Indriidae with redder pelage hues live in regions that experience large ranges in temperature (i.e., lower temperatures) (Figure 3, SI 24). Hue values across Indriidae exhibited moderate phylogenetic signal (0.53-0.67) (Table 2).

[Table 1 Here]

[Table 2 Here]

[Figure 2 Here]

[Figure 3 Here]

Within *Propithecus*

For the brightness PCA, the first PC explained ≈70% of the variation within *Propithecus* (SI 11). The highest loadings on PC1 were hindlimb, dorsal torso, and forelimb brightness (SI 12). We found a statistically significant and positive association between hair brightness and mean annual temperature (Table 1). Thus, darker pelage within *Propithecus* is associated with colder forests (Figure 2B). Brightness across Indriidae exhibited a high phylogenetic signal (0.90) (Table 1). For the hue PCA, the first three PCs explained ≈80% of the variation within *Propithecus* (SI 13, SI 14). The highest loadings were forelimb, dorsal torso, and hindlimb hue (PC1), cheek, ventral torso, and hindlimb hue (PC2), and crown hue (PC3) (SI 14). We found a

statistically significant relationship between PC2 and mean annual temperature, precipitation seasonality, precipitation of the wettest month, and body size (Table 3). Thus, redder hues within *Propithecus* are associated with lower precipitation seasonality (and higher rainfall). We found no statistically significant relationships between either PC1 or PC3 with the tested variables. There was low to moderate phylogenetic signal for hair hue within *Propithecus* (0.22-0.63) (Table 3).

[Table 3 Here]

Climate and body size effects on pelage density

<u>Across Indriidae</u>

Across Indriidae, the first three PCs explained ≈70% of the variation (SI 15, SI 16). The highest loadings were forelimb, hindlimb, and crown follicle density (PC1), ventral torso hair density and crown and hindlimb follicle density (PC2), and dorsal torso hair density (PC3) (SI 16). We found a statistically significant relationship between PC1 and precipitation seasonality as well as between PC3 and body size (Table 4). Specifically, the results suggest that in forests with high precipitation seasonality (dryer, open forests exposed to the sun) individuals exhibit an increase of follicle density on the limbs and crown (Figure 4). Also, smaller taxa have the highest hair density; and, larger individuals exhibit lower hair density on average (Figure 5). Pelage density across Indriidae exhibited low phylogenetic signal (0.21-0.33) (Table 4). We also found a statistically significant difference between hair density across body regions sampled (Table 5). Specifically, we found the crown and forelimbs exhibit the greatest hair density, and the ventral torso exhibits the least hair density (Figure 6A). However, we found no significant differences in

follicle density of regions sampled (Table 5, Figure 6B).

[Table 4 Here]

[Table 5 Here]

[Figure 4 Here]

[Figure 5 Here]

[Figure 6 Here]

Within *Propithecus*

Within *Propithecus*, the first three PCs explained ≈70% of the variation (SI 17, SI 18). The highest loadings were forelimb follicle density, crown hair density, and hindlimb follicle density (PC1), crown and hindlimb follicle density as well as hindlimb hair density (PC2), and ventral torso hair density (PC3) (SI 18). We found no statistically significant relationships between any PC value and either climate or body size variable (Table 6). Similarly to Indriidae, we detected significant differences between hair density and distinct body regions (SI 19), and no differences were detected among follicle density within *Propithecus* (SI 19, SI 20).

[Table 6 Here]

Polymorphic trichromacy and pelage hue variation

For the hue PCA using only a subset of the data from *Indri* and *Propithecus*, the first two PCs explained ≈66% of the variation (SI 21). The highest loadings to PC1 were forelimb, dorsal torso, and hindlimb hue, and the highest loadings to PC2 were cheek, ventral torso, and hindlimb hue (SI 22). From the simple linear model (lambda = 0), we found a statistically significant

relationship between PC1 with the difference in opsin spectral sensitivity ($p = 0.03$; $R^2 = .51$), but not with the overall number of alleles in the population (Table 7). Specifically, we found a significant negative linear relationship between spectral sensitivity and hue (Figure 7). Despite the smaller sample size of the PGLMM (lambda = 1), we detected a similar association that approaches statistical significance (pMCMC = 0.09) and only moderate phylogenetic signal (0.41) (SI 23).

[Table 7 Here]

[Figure 7 Here]

Discussion

Our overarching goals were to examine 1) if Indriidae pelage traits varied across distinct phylogenetic scales and 2) if multiple non-exclusive selective pressures would impact the same trait. We found support for both; distinct aspects of pelage color and density in Indriidae and sifakas (genus *Propithecus*) vary with climate, body size, and/or color vision.

Climate and body size effects on pelage brightness and hue

Our first sub-aim sought to uncover how climate and body size influenced pelage brightness and hue across two distinct scales (across a family [Indriidae] and within a genus [*Propithecus*]). Our results show distinct trends across scales regarding dark pelage (i.e., brightness). Specifically, across Indriidae, greater brightness is associated with greater precipitation seasonality (Table 1). Greater hue, in contrast, is associated with greater ranges in annual temperature across Indriidae (lower overall temperatures (SI 24)) (Table 2). Thus, black coats occur in regions of lower precipitation seasonality, and redder coats in areas that

experience larger ranges in temperature (Figure 2A, Figure 3). Generally, in Madagascar, low precipitation seasonality is strongly and negatively associated with high precipitation forests of the East (SI 24). The result for brightness in Indriidae follows Gloger's rule, predicting an increase in eumelanin (i.e., black pigments) (Delhey, 2017). Yet, within *Propithecus*, results indicate a relationship between brightness and mean annual temperature (Table 1). Thus, dark-haired sifakas are generally associated with colder regions, which serves as evidence of Bogert's rule (or the thermal melanism hypothesis) (Figure 2B) (Bogert, 1949).

Recent work highlights that discovering evidence for Bogert's or Gloger's rule may merely reflect differences in geographic space, scale, and climate gradients (Delhey et al., 2019). We show in this analysis that different effects can be detected across the primate coat, depending on the sampling scale. Additionally, the strength of selective pressures acting on pelage may also play a role in detecting either rule. For example, if the need to camouflage or avoid parasites is high, rainfall (which predicts Gloger's rule) may strongly affect pelage color (da Silva et al., 2016). This is because higher rainfall may also be associated with higher loads of parasites (Shearer and Ezenwa, 2020) or may indicate low light forested environments that enhance crypsis for dark animals (Caro, 2005; Delhey, 2018). In contrast, if the need for thermoregulation is high, temperature (which predicts Bogert's rule) may have a more substantial effect on pelage color than rainfall (Galván et al., 2018). It is hypothesized that black colors aid with thermoregulation in colder climates since they likely increase absorption of ultraviolet rays. While this has been documented widely in ectoderms and recently in birds (Bogert, 1949; Clusella Trullas et al., 2007; Bishop et al., 2016; Xing et al., 2016; Delhey et al., 2019), to date, our results serve as the first empirical evidence for Bogert's rule in mammals.

Both body size and phylogeny seem to have minimal impact on pelage color. First, body

size only influenced hair hue across the *Propithecus* clade and otherwise did not affect our coloration models across either scale (Table 2, Table 3). At first glance, smaller individuals seem to exhibit redder hues; however, this trend is driven mostly by *Propithecus* species on the western side of the island. This may indicate subtler variation between species that our analysis does not capture. However, these results may also reflect broader climatic trends, variations in color vision (addressed below), or is perhaps the product of our body size sampling methodology. Second, most of the coloration traits we sampled exhibited low to moderate phylogenetic signals. Our brightness models, on the other hand, had a high phylogenetic signal (≈0.80). Thus, brightness may implicate genetic drift (Losos, 2008; Revell et al., 2008). However, it is well established that primate coat color exhibits little to no phylogenetic signal and is a poor marker of phylogeny (Bell et al., 2021). An alternative explanation for such a high signal is that it is an "artificial" result from taxonomic inflation that merely reflects patterns of geographic variation (Kamilar and Muldoon, 2010).

Climate and body size effects on pelage density

Our second sub-aim sought to uncover how climate and body size influenced pelage hair and follicle density across two distinct scales (across a family [Indriidae] and within a genus [*Propithecus*]). We predicted that body size would affect density because these variables are associated across primates. Body size may also have been one of the factors influencing the reduction of the hairy coat in hominins (Schwartz and Rosenblum, 1981; Sandel, 2013). We found support for this prediction across Indriidae (Table 4). Specifically, higher hair density is associated with smaller body sizes (*Avahi*), and lower hair density is found in larger animals across Indriidae (Figure 4). One explanation for this result may be that interfollicular distance

442 increases as surface area increases, thus, decreasing hair density in larger animals (Sandel, 2013).
443 In addition, this relationship may provide thermoregulatory benefits since larger animals may
444 struggle more to dissipate heat (Schwartz and Rosenblum, 1981). Our models show that climate
445 also influences pelage variation across Indriidae. Limb and crown follicle density increases as
446 precipitation seasonality increases (i.e., shifting to dry open habitats) (Table 4; Figure 4).
447 Interestingly, the crown and forelimbs are also the regions that exhibit the highest degree of hair
448 density (Figure 6A)—but not follicle density (Figure 6B). Thus, there are likely two mechanisms
449 to increase density: (1) increase hair follicle density or (2) increase the number of hairs emerging
450 from each follicle. Since follicle density is determined in early embryogenesis, follicle density
451 may be more strongly genetically determined than hair density (which may be more plastic to
452 rapid environmental changes, such as seasonality) (Tapanes et al., 2021). Alternatively, follicle
453 density may be easier to measure without error and could be a more reliable estimate for
454 'hairiness.'

455 Nevertheless, the shift towards drier habitats exposed to more sun (such as Western spiny
456 thickets) leads to an increase in follicle density in the limbs and crown (Figure 4), where hair
457 density is already the highest of all regions (Figure 6A). Since all Indriidae are vertical clingers
458 and leapers, the crown and upper limbs are the most directly impacted by the sun's rays—as they
459 are known to hold up their arms while jumping bipedally. Thus, increased hair density in these
460 regions may aid individuals in this clade with protection from ultraviolet rays (and/or protect the
461 underlying skin from abrasion in spiny thickets). We consider this density pattern may help
462 prevent photolysis of folate, an essential metabolite in the formation of the embryonic neural
463 tube. Protection against folate leaching was likely a selection target in the evolution of high
464 melanization within the skin of humans living in high UV areas (Jablonski and Chaplin, 2000).

465 In humans, lower levels of folate (or folate deficiency) are also often significantly associated
466 with hair loss (Ertug, 2018; Almohanna et al., 2019), and folate may play a significant role
467 within the hair follicle (Durusoy et al., 2009). Since the skin of most Indriidae is already highly
468 melanized, it is not surprising that populations exposed to hotter environments and more direct
469 sun often have lighter coats (Figure 2B, Figure 3)—potentially to prevent overheating due to lack
470 of sweat glands. The pattern that emerges from this data may signal that variation in hair density
471 (i.e., higher hair density in the scalp) across the human body may have occurred early on as an
472 early mechanism to prevent folate leaching from key body regions exposed to direct UV rays.
473 This body hair pattern potentially preceded the evolution of "naked" skin and sweat glands.
474 Our data is also rare evidence supporting the body cooling hypothesis—from the
475 perspective of hair density in non-human primates. The body cooling hypothesis (Wheeler, 1985,
476 1992) argued that bipedal hominins evolved naked skin to allow for evaporative cooling.
477 However, Wheeler (1985, 1992) also argued as part of this hypothesis that bipedal hominins
478 likely retained hair on the crown and shoulders to protect those areas from UV exposure.
479 Indriidae, presenting similar postural locomotion to humans, exhibit follicle density increases in
480 their body regions most exposed to potential UV damage. Indriidae present a unique opportunity
481 to comparatively study potential tradeoffs between folate levels, hair density, hair color, and
482 thermoregulation across and within populations to clarify potential mechanisms driving this
483 pattern of hair variation in upright primates.
484 Our results indicate that body size is also likely contributing to hair density variation
485 (Figure 5). However, the smallest primates within the Indriidae clade are also nocturnal; larger-
486 bodied Indriidae are diurnal. Thus, "body size" is likely confounded by activity cycle. Our
487 results show that within *Propithecus* alone, there was no variation in hair density detected with

488 either body size or climate. This may be due to a smaller sample size available for *Propithecus*
489 density which we estimated would not pick up small effects (G* power analyses detailed in
490 methods). Alternatively, at smaller phylogenetic scales, other aspects of hair morphology that we
491 did not measure (e.g., overall shape, length, thickness) may directly relate to either climate or
492 body size best. For example, there are no differences in hair density between chimpanzees and
493 humans, but there are significant differences in gland density, sweat production, and overall hair
494 morphology (Kamberov et al., 2018). Hair and follicle density was likely one of a few aspects of
495 hair evolution that were potentially malleable and allowed rapid adaptation to changing climatic
496 environments for hominins. More research is needed across non-human and human primate hair
497 to understand why and how humans retained hair in the places they did (e.g., scalp, pubic)—a
498 critical part of the story in the evolution of our apparent "nakedness."
499
500 *Polymorphic trichromacy and pelage hue variation*
501 Our third sub-aim sought to understand the relationship between color vision and pelage
502 hue in diurnal genera. We found support for our prediction that populations with enhanced
503 capacity for trichromatic color vision would also contain individuals with redder pelage (*as*
504 *hypothesized in* (Sumner and Mollon, 2003)). Many primates are unique among placental
505 mammals in having trichromatic color vision, a feature that is thought to be advantageous for
506 foraging on "red" foods (i.e., ripe fruit, young leaves), detecting predators, and/or tracking
507 conspecifics (Kawamura et al., 2012; Surridge et al., 2003). Indeed, reddish skin coloration
508 observed in many primate species is thought to play a salient role in conspecific signaling for
509 primates (Moreira et al., 2019). However, previous support for the coevolution of red hair and
510 trichromacy in primates is mixed (Fernandez and Morris, 2007; Kamilar et al., 2013). Our results

indicate a significant positive relationship between hue ('redness') and measures of enhanced trichromacy in Indriidae (Table 7). The similarity in results between both models (lambda=0 vs. lambda=1) indicates a likely significant relationship between hue and opsin genotype variation in diurnal Indriidae. Specifically, red hues are more likely to occur when there is a more significant difference spectral sensitivity between opsin alleles (Figure 7), suggesting increased discriminability of such hues. Results across Indriidae, which exhibits more subtle inter- and intra-species variation in trichromacy than has been previously considered, suggests that there may be a more complex and nuanced coevolutionary relationship between red hair coloration in primates and trichromatic color vision that deserves further attention (Table 7).

Conclusions

Climate, body size, and color vision all impact hair variation across Indriidae, but the extent that each exerts its influence on the phenotype varies by sampled phylogenetic scale. These results have considerable implications for our understanding of primate (including human) hair evolution because it suggests that larger macro-scale trends detected across primates may not sufficiently explain variation within a genus, species, or population. Understanding wild non-human primate hair can also potentially help shed light on the evolution of hominin hair. Further work on primate hair should sample across smaller geographic or phylogenetic scales and from diverse non-human and human populations.

Acknowledgments

We thank the American Museum of Natural History, the Smithsonian National Museum of Natural History, and Harvard University's Museum of Comparative Zoology. Special thanks to museum staff that helped with *Propithecus* collections, including Ian Tattersall, Darrin Lunde, Mark Omura, Eleanor Hoeger, and Marisa Surovy. We also thank the Government of Madagascar (Ministry of the Environment and Sustainable Development), SADABE, Madagascar Biodiversity Partnership (MBP), Omaha Zoo, the University of Antananarivo, and Anthropobiologie et Développement for facilitation and partnership.

551 **References**

552 Allen, W.L., Higham, J.P., 2013. Analyzing visual signals as visual scenes. American journal of
553 primatology. 75, 664–82.

554 Almohanna, H.M., Ahmed, A.A., Tsatalis, J.P., Tosti, A., 2019. The Role of Vitamins and
555 Minerals in Hair Loss : 51–70.

556 Avram, M.R., Rogers, N.E., 2009. The use of low-level light for hair growth: Part i. Journal of
557 Cosmetic and Laser Therapy. 11, 110–117.

558 Barrett, R.D.H., Laurent, S., Mallarino, R., Pfeifer, S.P., Xu, C.C.Y., Foll, M., Wakamatsu, K.,
559 Duke-Cohan, J.S., Jensen, J.D., Hoekstra, H.E., 2019. Linking a mutation to survival in wild
560 mice. Science. 363, 499–504.

561 Bell, R.B., Bradley, B.J., Kamilar, J.M., 2021. The Evolutionary Ecology of Primate Hair
562 Coloration : A Phylogenetic Approach.

563 Bergman, T.J., Beehner, J.C., 2008. A simple method for measuring colour in wild animals:
564 validation and use on chest patch colour in geladas (Theropithecus gelada). Biological
565 Journal of the Linnean Society. 94, 231–240.

566 Best, A., Lieberman, D., Kamilar, J., 2019. Diversity and evolution of human eccrine sweat
567 gland density. Journal of Thermal Biology. 84, 331–338.

568 Bishop, T.R., Robertson, M.P., Gibb, H., van Rensburg, B.J., Braschler, B., Chown, S.L., Foord,
569 S.H., Munyai, T.C., Okey, I., Tshivhandekano, P.G., Werenkraut, V., Parr, C.L., 2016. Ant
570 assemblages have darker and larger members in cold environments. Global Ecology and
571 Biogeography. 25, 1489–1499.

572 Bogert, C.M., 1949. Thermoregulation in reptiles, a factor in evolution. Evolution. 3, 195–211.

573 Bradley, B.J., Walsh, S., Nishimura, A., Karlsson, J., Kamilar, J.M., 2014. The evolution of

primate pelage: Morphological analysis of museum research skins. In: Program of the 83rd Annual Meeting of the American Association of Physical Anthropologists.

Caro, T., 2005. The adaptive significance of coloration in mammals. BioScience. 55, 125.

Chaplin, George, Jablonski, Nina G., Cable, T.N., 1994. Physiology, thermoregulation and bipedalism. Journal of Human Evolution. 27, 497–510.

Clusella Trullas, S., van Wyk, J.H., Spotila, J.R., 2007. Thermal melanism in ectotherms. Journal of Thermal Biology. 32, 235–245.

Cuthill, I.C., Allen, W.L., Arbuckle, K., Caspers, B., Chaplin, G., Hauber, M.E., Hill, G.E., Jablonski, N.G., Jiggins, C.D., Kelber, A., Mappes, J., Marshall, J., Merrill, R., Osorio, D., Prum, R., Roberts, N.W., Roulin, A., Rowland, H.M., Sherratt, T.N., Skelhorn, J., Speed, M.P., Stevens, M., Stoddard, M.C., Stuart-Fox, D., Talas, L., Tibbetts, E., Caro, T., 2017. The biology of color. Science. 357.

da Silva, L.G., de Oliveira, T.G., Kasper, C.B., Cherem, J.J., Moraes, E.A., Paviolo, A., Eizirik, E., 2016. Biogeography of polymorphic phenotypes: Mapping and ecological modelling of coat colour variants in an elusive Neotropical cat, the jaguarundi (Puma yagouaroundi). Journal of Zoology. 299, 295–303.

Delhey, K., 2017. Gloger's rule. Current Biology. 27, R689–R691.

Delhey, K., 2018. Darker where cold and wet: Australian birds follow their own version of Gloger's rule. Ecography. 41, 673–683.

Delhey, K., Dale, J., Valcu, M., Kempenaers, B., 2019. Reconciling ecogeographical rules: rainfall and temperature predict global colour variation in the largest bird radiation. Ecology Letters. 22, 726–736.

Durusoy, C., Ozenli, Y., Adiguzel, A., Budakoglu, I.Y., Tugal, O., Arikan, S., Uslu, A., 2009.

The role of psychological factors and serum zinc , folate and vitamin B 12 levels in the aetiology of trichodynia : a case – control study. 789–792.

Dutton, A., Christopher, J., Randall, E., 2003. Biomedical Evaluation of Free-Ranging Ring-Tailed Lemurs (Lemur Catta) in Tsimanampetsotsa Strict Nature Reserve, Madagascar. Journal of Zoo and Wildlife Medicine. 34, 16–24.

Ertug, E.Y., 2018. Research Article Reduced ferritin, folate, and vitamin B12 levels in female patients diagnosed with telogen effluvium. 1, 0–2.

Faul, F., Erdfelder, E., Buchner, A., Lang, A.G., 2009. Statistical power analyses using G*Power 3.1: Tests for correlation and regression analyses. Behavior Research Methods. 41, 1149–1160.

Fernandez, A.A., Morris, M.R., 2007. Sexual selection and trichromatic color vision in primates: Statistical support for the preexisting-bias hypothesis. American Naturalist. 170, 10–20.

Fratto, M.A., Davis, A.K., 2011. Do black-furred animals compensate for high solar absorption with smaller hairs? A test with a polymorphic squirrel species. Current Zoology. 57, 731–736.

Galván, I., Rodríguez-Martínez, S., Carrascal, L.M., 2018. Dark pigmentation limits thermal niche position in birds. Functional Ecology. 32, 1531–1540.

Hadfield, J.D., 2010. MCMC methods for multi-response generalized linear mixed models: The MCMCglmm R package. Journal of Statistical Software. 33, 1–22.

Hansen, T.F., Orzack, S.H., 2005. Assessing Current Adaptation and Phylogenetic Inertia As Explanations of Trait Evolution: the Need for Controlled Comparisons. Evolution. 59, 2063.

Herrera, J.P., Dávalos, L.M., 2016. Phylogeny and Divergence Times of Lemurs Inferred with Recent and Ancient Fossils in the Tree. Systematic Biology. 65, 772–791.

620 Hijmans, R.J., Etten, J. V., 2012. Raster: Geographic analysis and modeling with raster data. R
621 package version 2.0-12.
622 Hoekstra, H.E., Krenz, J.G., Nachman, M.W., 2005. Local adaptation in the rock pocket mouse
623 (Chaetodipus intermedius): Natural selection and phylogenetic history of populations.
624 Heredity. 94, 217–228.
625 Irwin, M.T., Junge, R.E., Raharison, J.L., Samonds, K.E., 2010. Variation in physiological health
626 of diademed sifakas across intact and fragmented forest at Tsinjoarivo, eastern Madagascar.
627 American Journal of Primatology. 72, 1013–1025.
628 Jablonski, N.G., Chaplin, G., 2000. The evolution of human skin coloration. Journal of Human
629 Evolution. 39, 57–106.
630 Jacobs, R.L., MacFie, T.S., Spriggs, A.N., Baden, A.L., Morelli, T.L., Irwin, M.T., Lawler, R.R.,
631 Pastorini, J., Mayor, M., Lei, R., Culligan, R., Hawkins, M.T.R., Kappeler, P.M., Wright,
632 P.C., Louis, E.E., Mundy, N.I., Bradley, B.J., 2017. Novel opsin gene variation in
633 largebodied, diurnal lemurs. Biology Letters. 13, 1–6.
634 Jacobs, R.L., Spriggs, A.N., MacFie, T.S., Baden, A.L., Irwin, M.T., Wright, P.C., Louis, E.E.,
635 Lawler, R.R., Mundy, N.I., Bradley, B.J., 2016. Primate genotyping via high resolution melt
636 analysis: rapid and reliable identification of color vision status in wild lemurs. Primates. 57,
637 541–547.
638 Jacobs, R.L., Veilleux, C.C., Louis, E.E., Herrera, J.P., Hiramatsu, C., Frankel, D.C., Irwin,
639 M.T., Melin, A.D., Bradley, B.J., 2019. Less is more: lemurs (Eulemur spp.) may benefit
640 from loss of trichromatic vision. Behavioral Ecology and Sociobiology. 73.
641 Kamberov, Y.G., Guhan, S.M., DeMarchis, A., Jiang, J., Wright, S.S., Morgan, B.A., Sabeti,
642 P.C., Tabin, C.J., Lieberman, D.E., 2018. Comparative evidence for the independent

643 evolution of hair and sweat gland traits in primates. Journal of Human Evolution. 125, 99–
644 105.
645 Kamilar, J.M., Bradley, B.J., 2011. Interspecific variation in primate coat colour supports
646 Gloger's rule. Journal of Biogeography. 38, 2270–2277.
647 Kamilar, J.M., Cooper, N., 2013. Phylogenetic signal in primate behaviour, ecology and life
648 history. Philosophical transactions of the Royal Society of London. Series B, Biological
649 sciences. 368, 20120341.
650 Kamilar, J.M., Heesy, C.P., Bradley, B.J., 2013. Did trichromatic color vision and red hair color
651 coevolve in primates? American Journal of Primatology.
652 Kamilar, J.M., Muldoon, K.M., 2010. The climatic niche diversity of Malagasy primates: A
653 phylogenetic perspective. PLoS ONE. 5.
654 Kawamura, S., Hiramatsu, C., Melin, A.D., Schaffner, C.M., Aureli, F., Fedigan, L.M., 2012.
655 Polymorphic Color Vision in Primates: Evolutionary Considerations. 93–120.
656 Kendal, D., Hauser, C.E., Garrard, G.E., Jellinek, S., Giljohann, K.M., Moore, J.L., 2013.
657 Quantifying Plant Colour and Colour Difference as Perceived by Humans Using Digital
658 Images. PLoS ONE. 8, 1–11.
659 King, T., Rakotonirina, L.H.F., Rakotoarisoa, A.H., Razafindramanana, J., Ratsimbazafy, J.,
660 2014. Distributional limits and melanism in the south-west of the range of the crowned
661 sifaka (Propithecus coronatus), Madagascar. Primate Conservation. 28, 55–64.
662 Lasisi, T., Ito, S., Wakamatsu, K., Shaw, C.N., 2016. Quantifying variation in human scalp hair
663 fiber shape and pigmentation. American Journal of Physical Anthropology. 160, 341–352.
664 Lehman, S.M., 2007. Ecological and phylogenetic correlates to body size in the Indriidae.
665 International Journal of Primatology. 28, 183–210.

Lewis, R.J., Van Schaik, C.P., 2007. Bimorphism in male verreaux's sifaka in the Kirindy Forest of Madagascar. International Journal of Primatology. 28, 159–182.

Losos, J.B., 2008. Phylogenetic niche conservatism, phylogenetic signal and the relationship between phylogenetic relatedness and ecological similarity among species. Ecology Letters. 11, 995–1003.

Lynch, M., 1991. Methods for the analysis of comparative data in evolutionary biology. Evolution. 45, 1065–1080.

McLean, M.J., Bishop, P.J., Nakagawa, S., 2013. Assessing the Patterns of Evolution in Anuran Vocal Sexual Signals. Evolutionary Biology. 40, 141–149.

Mittermeier, Russell A., Louis, Jr., Edward E., Richardson, M., Schwitzer, C., Langrand, O., Rylands, Anthony B., Hawkins, Frank, Rajaobelina, S., Ratsimbazafy, J., Rasoloarison, R., Roos, C., Kappeler, P.M., MacKinnon, K.C., 2010. Lemurs of Madagascar, 3rd ed.

Moreira, L.A.A., Duytschaever, G., Higham, J.P., Melin, A.D., 2019. Platyrrhine color signals: New horizons to pursue. Evolutionary Anthropology. 28, 236–248.

Norton, H.L., Edwards, M., Krithika, S., Johnson, M., Werren, E.A., Parra, E.J., 2016. Quantitative assessment of skin, hair, and iris variation in a diverse sample of individuals and associated genetic variation. American Journal of Physical Anthropology. 160, 570–581.

Osorio, D., Smith, A.C., Vorobyev, M., Buchanan-Smith, H.M., 2004. Detection of fruit and the selection of primate visual pigments for color vision. American Naturalist. 164, 696–708.

Paus, R., Foitzik, K., 2004. In search of the "hair cycle clock": A guided tour. Differentiation. 72, 489–511.

Pebesma, E.J., Bavand, R.S., n.d. Classes and methods for spatial data in R. R News. 5, 9–13.

Petter, J.J., Peyrieras, A., 1972. Melanization in the genus Propithecus Malagasey Lemur. Journal of Human Evolution. 1, 379–388.

Post, P.W., Szabó, G., Keeling, M.E., 1975. A quantitative and morphological study of the pigmentary system of the chimpanzee with the light and electron microscope. American Journal of Physical Anthropology. 43, 435–443.

Rakotonirina, H., Kappeler, P.M., Fichtel, C., 2017. Evolution of facial color pattern complexity in lemurs. Scientific Reports. 7, 1–11.

Rakotonirina, L.H.F., Randriantsara, F., Rakotoarisoa, A.H., Rakotondrabe, R., Razafindramanana, J., Ratsimbazafy, J., King, T., 2014. A preliminary assessment of sifaka (propithecus) distribution, chromatic variation and conservation in Western Central Madagascar. Primate Conservation. 28, 43–53.

Ramírez-Delgado, V.H., Sanabria-Urbán, S., Serrano-Meneses, M.A., Cueva del Castillo, R., 2016. The converse to Bergmann's rule in bumblebees, a phylogenetic approach. Ecology and Evolution. 6, 6160–6169.

Revell, L.J., Harmon, L.J., Collar, D.C., 2008. Phylogenetic signal, evolutionary process, and rate. Systematic biology. 57, 591–601.

Rowe, N., 1996. The pictoral guide to the living primates. Pagonias Press, East Hampton.

Sambrook, J., Fritch, E., Maniatus, T., 1989. Molecular cloning: a laboratory manual., 2nd ed. ed. Cold Spring Harbor Press, New York.

Sandel, A.A., 2013. Brief communication: Hair density and body mass in mammals and the evolution of human hairlessness. American Journal of Physical Anthropology. 152, 145–150.

Santana, S.E., Alfaro, J.L., Noonan, A., Alfaro, M.E., 2013. Adaptive response to sociality and

ecology drives the diversification of facial colour patterns in catarrhines. Nature Communications. 4, 1–7.

Santana, S.E., Lynch Alfaro, J., Alfaro, M.E., 2012. Adaptive evolution of facial colour patterns in Neotropical primates. Proceedings. Biological sciences / The Royal Society. 279, 2204–11.

Schmidt, M., 2011. Locomotion and postural behaviour. Advances in Science and Research. 5, 23–39.

Schwartz, G.G., Rosenblum, L.A., 1981. Allometry of primate hair density and the evolution of human hairlessness. American Journal of Physical Anthropology. 55, 9–12.

Seibert, H.C., Steggerda, M., 1999. The Size and Shape of human head hair - Along Its Shaft. The Journal of Heredity. 302–304.

Shearer, C.L., Ezenwa, V.O., 2020. Rainfall as a driver of seasonality in parasitism. International Journal for Parasitology: Parasites and Wildlife. 12, 8–12.

Spriggs, A.N., 2017. Evolution of Lemur Color Evolution. University at Albany, State University of New York.

Steggerda, M., Seibert, H.C., 1941. Size and shape of head hair from six racial groups. Journal of Heredity. 32, 315–318.

Stevens, M., Párraga, C.A., Cuthill, I.C., Partridge, J.C., Troscianko, T.S., 2007. Using digital photography to study animal coloration. Biological Journal of the Linnean Society. 90, 211–237.

Stevens, M., Stoddard, M.C., Higham, J.P., 2009. Studying primate color: towards visual system-dependent methods. International Journal of Primatology. 30, 893–917.

Sumner, P., Mollon, J.D., 2003. Colors of primate pelage and skin: Objective assessment of

735 conspicuousness. American Journal of Primatology. 59, 67–91.
736 Surridge, A.K., Osorio, D., Mundy, N.I., 2003. Evolution and selection of trichromatic vision in
737 primates. Trends in Ecology and Evolution. 18, 198–205.
738 Tapanes, Elizabeth, Kamilar, Jason M, Bradley, B.J., 2021. Molecular and Cellular Processes of
739 Pelage Growth and Pigmentation in Primate Evolution. In: Evolutionary Cell Processes in
740 Primates. pp. 1–33.
741 Tapanes, E., Irwin, M., Spriggs, Amanda Nicole, Kamilar, Jason M., Bradley, B.J., 2018. Subtle
742 sexual dichromatism and dimorphism detected in wild Propithecus diadema. In: The 87th
743 Annual Meeting of the American Association of Physical Anthropologists.
744 Tattersall, I., 1986. Notes on the distribution and taxonomic status of some species of
745 Propithecus In Madagascar. Folia Primatologica. 46, 51–63.
746 Villemereuil, P. de, Nakagawa, S., 2014. General quantitative genetic methods for comparative
747 biology. In: Modern Phylogenetic Comparative Methods and Their Application in
748 Evolutionary Biology. pp. 287–304.
749 Wheeler, P.E., 1985. The loss of functional body hair in man: the influence of thermal
750 environment, body form and bipedality. Journal of Human Evolution. 14, 23–28.
751 Wheeler, P.E., 1992. The influence of the loss of functional body hair on the water budgets of
752 early hominids. Journal of Human Evolution. 23, 379–388.
753 Winters, S., Allen, W., Higham, J., 2019. The structure of species discrimination signals across a
754 primate radiation. 1–28.
755 Xing, S., Bonebrake, T.C., Tang, C.C., Pickett, E.J., Cheng, W., Greenspan, S.E., Williams, S.E.,
756 Scheffers, B.R., 2016. Cool habitats support darker and bigger butterflies in Australian
757 tropical forests. Ecology and Evolution. 6, 8062–8074.

Figures

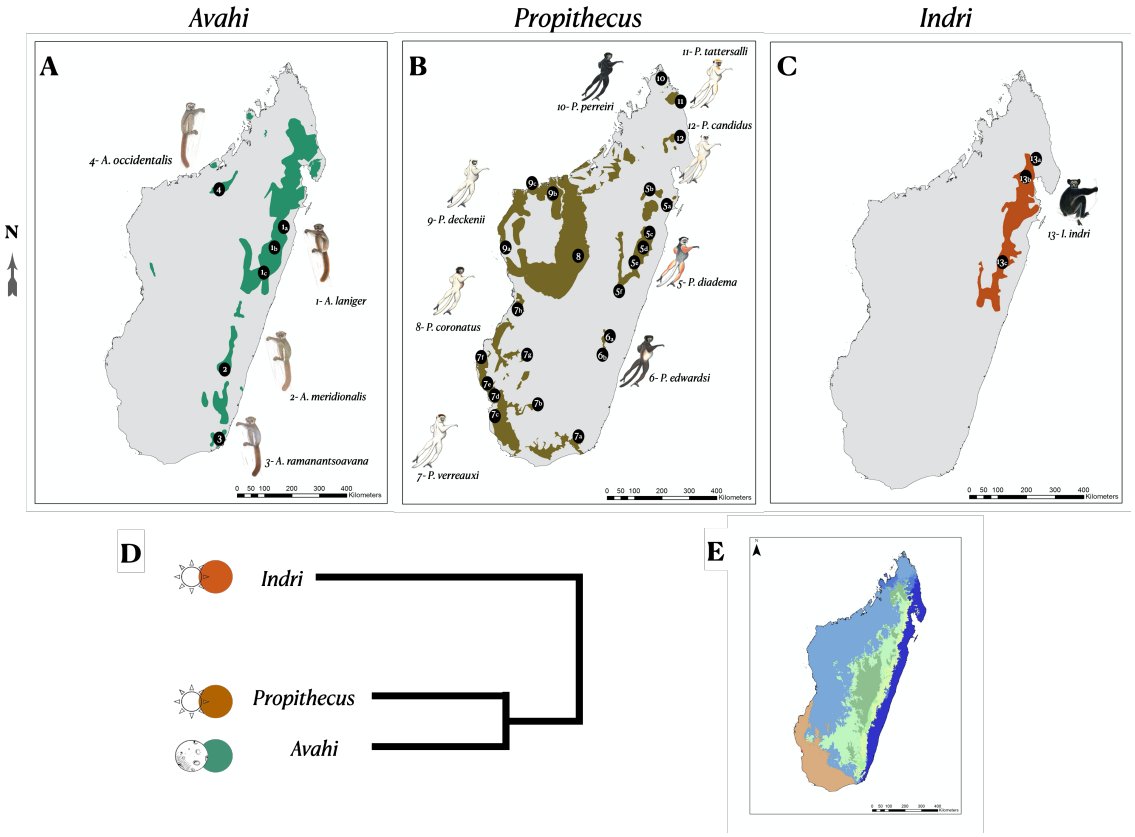

Figure 1 Indriidae species ranges and sampling localities for (A) *Avahi*, (B) *Propithecus*, and (C) *Indri*; along with a (D) cladogram, and (E) Koppen-climate zones that span the genera's distribution.

Key: *Avahi* spp. = (1a) Betampona, (1b) Sihanaka forest, (1c) Andasibe, (2) Forest west of Fort Dauphin, (3) Vondrozo, (4) Ankarafatsika; *Propithecus* spp. = (5a) Betampona, (5b) Zahamahena, (5c) Didy, (5d) Sihanaka forest, (5e) forest patch near Andasibe, (5f) Tsinjoarivo (eastern and western), (6a) Nandihizana, (6b) East of Farohny River, (7a) Mandrare Valley, (7b) Bevala East, (7c) Tsinanampetsotsa, (7d) Lower Ifaty, (7e) Ifaty, (7f) Lake Ihortry, (7g) Ankazoabo West, (7h) Upper Tsirbihina River, (8) Ambararatabe, (9a) Tsingy de Bemaraha, (9b) Tsingy de Namoraka, (9c) Baie de Baly Nat Park, (10) Reserve of Analamerana, (11) Forest fragment near Daraina, (12) Anjanaharibe-Sud Reserve; *Indri* indri = (13a) Anjanaharibe-Sud Reserve, (13b) 40 km West of Maroantsetra, (13c) Sihanaka forest

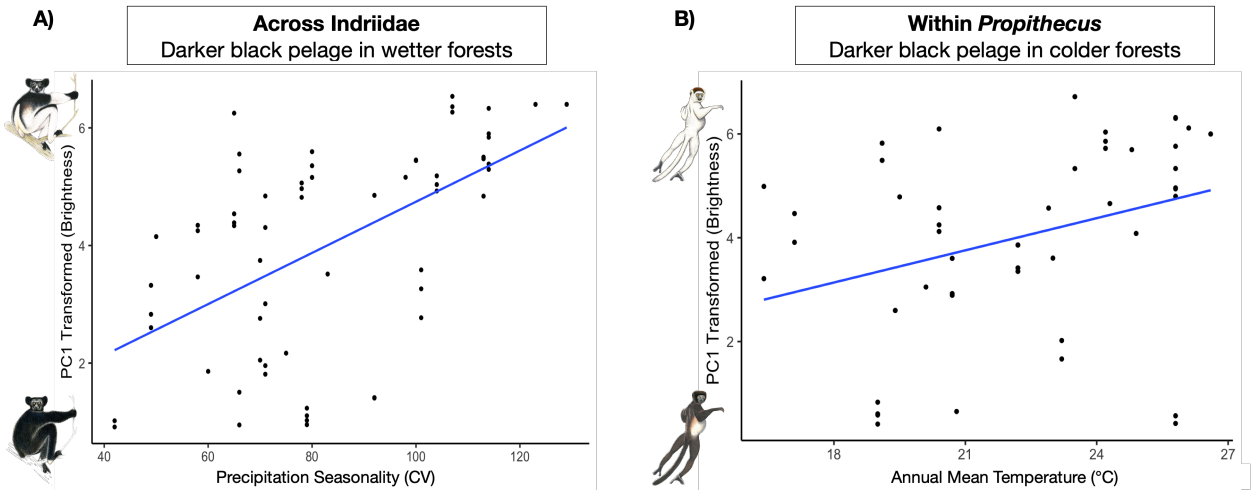

Figure 2 Plot of brightness across (A) the entire Indriidae family, in association with precipitation Seasonality (CV) (showing adherence to Gloger's Rule), and (B) only within the *Propithecus* genus, in association with Annual Mean Temperature (°C) (showing adherence to Bogert's Rule).

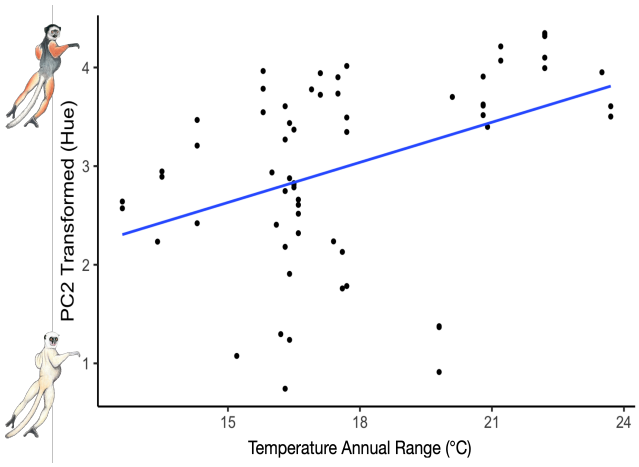

Figure 3 Plot of pelage hue trends across (A) the entire Indriidae family, in association with temperature annual range (°C) (showing adherence to Gloger's Rule). Results are similar within *Propithecus*.

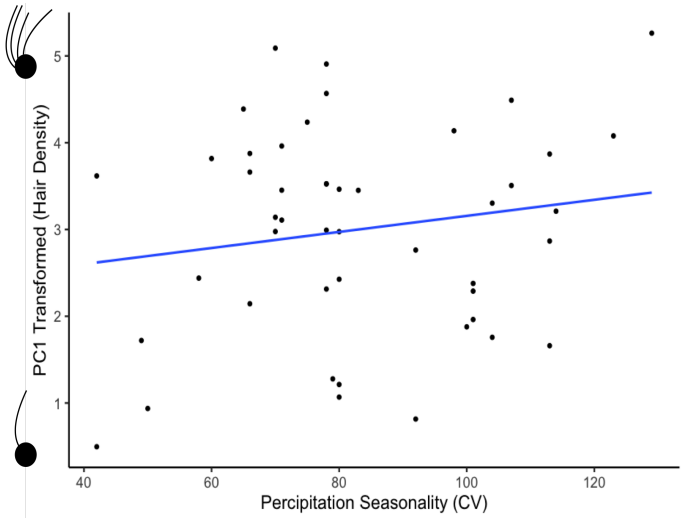

Figure 4 Plot of hair density trends. The relationship between PC1 and precipitation seasonality (CV) is significantly associated with hair density on the limbs and crown across the Indriidae family. Lower PC1 values are associated with lower hair density on the limbs and crown.

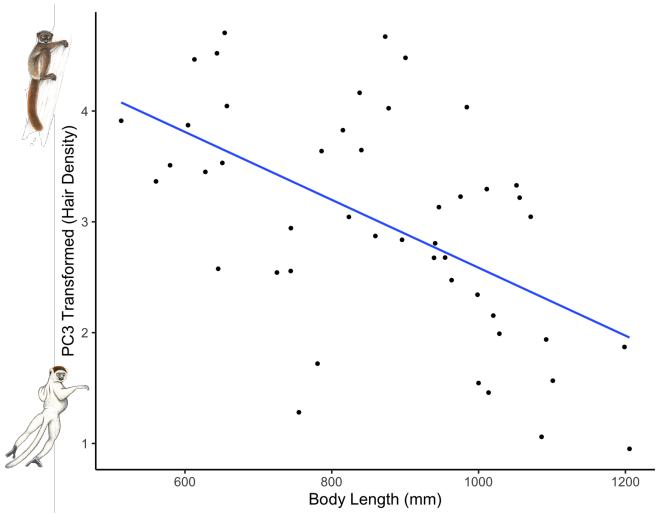

Figure 5 Plot of hair density trends. The relationship between PC3 and body length (capturing length, in mm) is significantly associated with hair density on the dorsal torso across Indriidae. Lower PC3 values are associated with lower hair density across the dorsal torso.

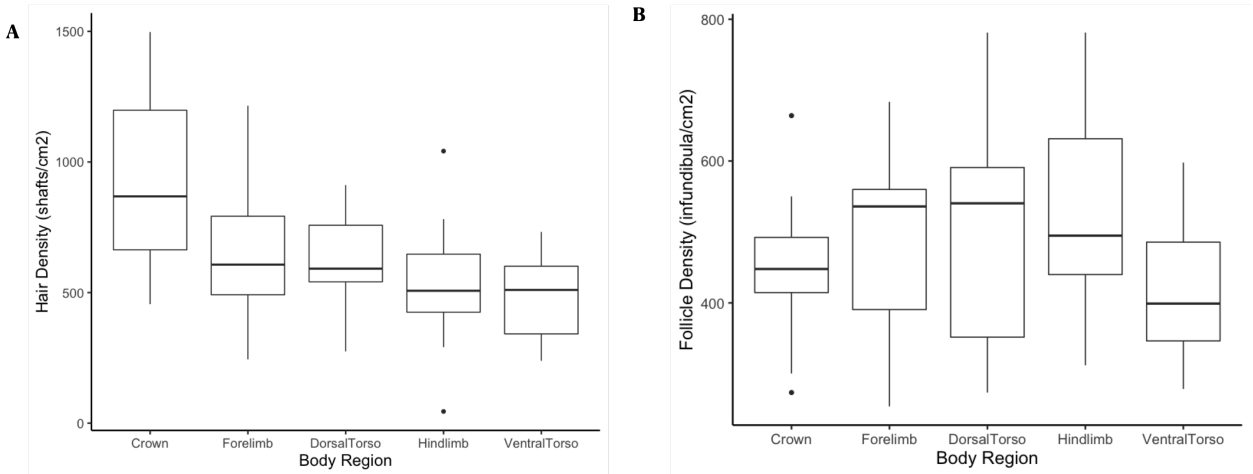

Figure 6 Boxplots illustrating variation in (A) hair density and (B) follicle density across body regions, for Indriidae. Black lines represent the average, and black dots represent outliers.

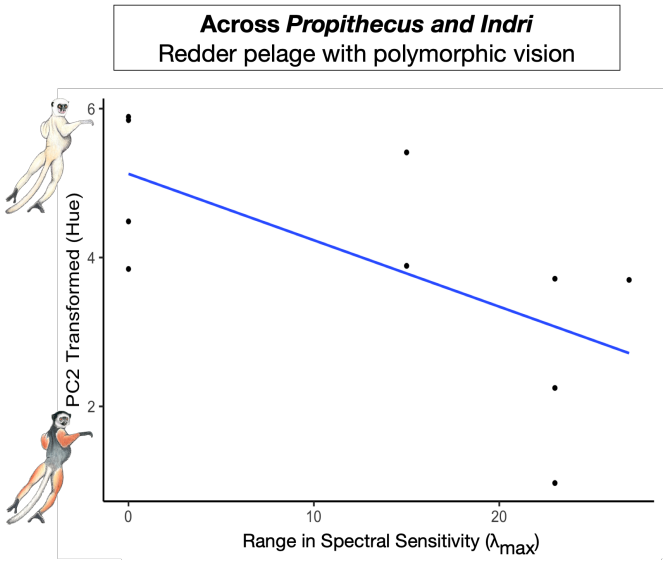

Figure 7 Plot of pelage hue trends across diurnal *Propithecus* and *Indri* genera, in association with the range (i.e., difference) in opsin peak spectral sensitivity.

Table 1 Results of PGLMMs predicting hair brightness (RGB averages) across all Indriidae taxa and only within *Propithecus*

Variable	Mean Est.	Lower CI	Upper CI	ESS	P MCMC
Across Indriidae (PC1; $H^2 = 0.700$)					
Intercept	-5.914	-16.017	4.438	9,000	0.251
BIO01	-0.543	-1.491	0.405	9,295	0.254
BIO04	0.896	-0.523	2.315	9,000	0.216
BIO07	-0.388	-2.179	1.459	9,000	0.670
BIO13	0.297	-0.179	0.772	9,000	0.203
BIO15	0.728	0.034	1.484	9,000	**0.050**
Body size	0.011	-0.722	0.723	9,000	0.980
Within *Propithecus* (PC1; $H^2 = 0.902$)					
Intercept	0.675	-8.993	10.320	9,000	0.886
BIO01	-1.303	-2.068	-0.578	9,000	**0.002**
BIO04	-0.489	-1.904	0.931	9,000	0.491
BIO07	0.592	-1.024	2.088	9,000	0.444
BIO13	0.002	-0.439	0.398	9,000	0.981
BIO15	0.362	-0.304	0.981	9,000	0.274
Body size	0.531	-0.061	1.106	9,000	$0.074^{!}$

Bold values indicate $p < 0.05$, $^{!}$ indicates $p < 0.10$, H^2 is akin to phylogenetic signal

829 **Table 2** Results of PGLMMs predicting hair hue (RG ratio values) across all Indriidae taxa

Variable	Mean Est.	Lower CI	Upper CI	ESS	P MCMC
PC1; $H^2 = 0.667$					
Intercept	-6.005	-16.249	4.025	9,114	0.243
BIO01	-0.529	-1.484	0.400	9,000	0.268
BIO04	0.903	-0.436	2.379	9,000	0.210
BIO07	-0.377	-2.242	1.335	9,000	0.676
BIO13	0.298	-0.159	0.770	8,684	0.216
BIO15	0.722	-0.015	1.413	9,000	0.051[!]
Body size	0.012	-0.689	0.746	9,000	0.970
PC2; $H^2 = 0.530$					
Intercept	3.081	-5.331	11.610	9,000	0.480
BIO01	0.187	-0.619	1.046	9,000	0.657
BIO04	-0.960	-2.143	0.220	9,000	0.103
BIO07	1.675	0.222	3.195	9,000	**0.026**
BIO13	-0.212	-0.592	0.168	8,953	0.258
BIO15	-0.486	-1.083	0.115	9,000	0.112
Body size	0.155	-0.462	0.750	9,000	06.09

830 Bold values indicate significance below 0.05, [!] indicates $p < 0.10$, H^2 is akin to phylogenetic

831 signal.

832

833

834

835

Table 3 Results of PGLMMs predicting hair hue (RG ratio values) within the *Propithecus* genus

Variable	Mean Est.	Lower CI	Upper CI	ESS	P MCMC
PC1; $H^2 = 0.637$					
Intercept	-0.552	-18.757	18.397	9,347	0.956
BIO01	-0.021	-2.034	1.851	9,000	0.974
BIO04	-0.403	-2.744	2.072	9,000	0.705
BIO07	0.109	-3.216	3.227	9,000	0.927
BIO13	-0.252	-1.118	0.599	9,000	0.549
BIO15	0.571	-0.989	2.057	9,000	0.461
Body size	0.381	-1.260	1.926	9,357	0.637
PC2; $H^2 = 0.520$					
Intercept	1.839	-7.905	11.710	9,000	0.714
BIO01	1.432	0.492	2.392	9,000	**0.004**
BIO04	-1.223	-2.593	0.164	9,000	0.079[!]
BIO07	1.158	-0.672	2.878	9,000	0.195
BIO13	-0.450	-0.881	0.018	9,000	**0.048**
BIO15	-1.092	-1.870	-0.319	9,000	**0.008**
Body size	0.801	0.074	1.547	9,000	**0.034**
PC3; $H^2 = 0.224$					
Intercept	3.427	-10.922	19.147	9,000	0.618
BIO01	-0.430	-2.037	1.143	9,000	0.583
BIO04	0.135	-1.603	2.164	9,000	0.932
BIO07	-0.739	-3.181	1.703	9,000	0.551
BIO13	-0.011	-0.701	0.618	9,000	0.963
BIO15	-0.015	-1.168	1.230	9,000	0.971
Body size	-0.151	-1.192	1.435	9,000	0.828

Bold values indicate significance below 0.05, [!] indicates $p < 0.10$, H^2 is akin to phylogenetic signal.

848 **Table 4** Results of PGLMMs predicting hair and follicle density across all Indriidae taxa

Variable	Mean Est.	Lower CI	Upper CI	ESS	P MCMC
PC1; $H^2 = 0.222$					
Intercept	-6.478	-22.987	18.456	9,456	0.401
BIO01	-0.036	-1.368	1.366	9,000	0.961
BIO04	0.770	-0.673	2.228	9,000	0.278
BIO07	-1.093	-3.262	1.047	9,434	0.314
BIO13	0.523	-0.085	1.190	9,000	0.101
BIO15	1.232	0.185	2.255	9,290	**0.020**
Body size	-0.275	-1.326	0.770	9,339	0.597
PC2; $H^2 = 0.217$					
Intercept	0.256	-15.042	16.829	9,000	0.981
BIO01	0.175	-1.238	1.587	9,000	0.812
BIO04	0.150	-1.334	1.643	9,000	0.835
BIO07	-0.990	-3.299	1.243	9,000	0.375
BIO13	0.110	-0.523	0.806	9,000	0.736
BIO15	0.518	-0.550	1.585	9,765	0.331
Body size	-0.161	-1.266	0.922	8,309	0.760
PC3; $H^2 = 0.330$					
Intercept	10.259	-0.399	20.576	9,000	0.057[1]
BIO01	-0.259	-1.175	0.700	9,000	0.602
BIO04	0.071	-0.953	1.056	9,307	0.876
BIO07	-0.129	-1.643	1.413	9,000	0.853
BIO13	-0.337	-0.772	0.081	9,000	0.123
BIO15	0.438	-0.276	1.164	9,908	0.228
Body size	-1.265	-2.012	-0.514	9,000	**0.002**

849 Bold values indicate significance below 0.05, [1] indicates $p < 0.10$, H^2 is akin to phylogenetic signal.

850

851

852 **Table 5** Summary of ANOVA examining hair and follicle density variation across distinct body

853 regions for Indriidae

	DF	Sum Sq.	Mean Sq.	F value	P value
Hair density					
Body Region	4	1458536	364634	5.808	**< 0.0001**
Residuals	60	3766879	62781		
Follicle density					
Body Region	4	108592	27148	1.524	0.207
Residuals	60	1068659	17811		

854
855
856
857
858
859
860
861
862
863
864
865
866
867
868
869

870 **Table 6** Results of PGLMMs predicting hair and follicle density within the *Propithecus* genus

Variable	Mean Est.	Lower CI	Upper CI	ESS	P MCMC
PC1; $H^2 = 0.270$					
Intercept	8.876	-9.863	26.645	9,000	0.315
BIO01	1.116	-0.473	2.668	9,280	0.160
BIO04	0.032	-1.716	1.724	7,868	0.987
BIO07	0.562	-2.273	3.088	9,000	0.671
BIO13	-0.113	-0.798	0.580	8,822	0.746
BIO15	-0.796	-1.978	0.296	9,000	0.167
Body size	-1.173	-2.607	0.333	9,000	0.111
PC2; $H^2 = 0.190$					
Intercept	9.252	-17.259	37.827	9,000	0.494
BIO01	1.437	-0.749	3.688	9,000	0.192
BIO04	0.351	-2.135	2.597	9,000	0.760
BIO07	-0.042	-3.693	3.627	9,571	0.988
BIO13	-0.090	-1.141	0.898	9,356	0.862
BIO15	-0.508	-2.082	1.157	9,000	0.530
Body size	-1.632	-3.695	0.666	9,000	0.134
PC3; $H^2 = 0.279$					
Intercept	-12.391	-31.523	5.691	9,000	0.186
BIO01	0.766	-0.815	2.345	9,000	0.330
BIO04	1.090	-0.802	2.988	9,000	0.224
BIO07	-1.264	-4.442	1.564	9,000	0.382
BIO13	0.437	-0.282	1.117	9,000	0.219
BIO15	0.309	-0.864	1.559	9,000	0.606
Body size	0.738	-0.698	2.194	9,000	0.310

871 Bold values indicate significance below 0.05, [1] indicates $p < 0.10$, H^2 is akin to phylogenetic signal.

872

873
874
875
876
877
878
879
880
881
882
883
884
885
886
887
888

889 **Table 7** Summary of linear models examining pelage coloration against difference in opsin peak
890 spectral sensitivity, using hue (PC1) scores of individuals across a subset of 10 sampling
891 locations

	Estimate	**Std. Error**	**T value**	**P value**
PC1				
[Intercept]	-1.529	1.611	-0.949	0.374
Difference in Spectral Sensitivity	-0.234	0.089	-2.630	**0.034**
Number of Opsin Alleles	2.635	1.501	1.746	0.124

892 SE: 1.05 on 7 degrees of freedom; R^2= 0.516, F = 5.801 on 2 and 7 degrees of freedom; p = 0.033. Bold values
893 indicate significance below 0.05.

894
895
896
897